Available online at www.sciencedirect.com

SCIENCE DIRECT®

Cement and Concrete Research 35 (2005) 11–18

CEMENT AND CONCRETE RESEARCH

Properties of confined fibre-reinforced concrete under uniaxial compressive impact

Piti Sukontasukkul[a,1], Sidney Mindess[b,*], Nemkumar Banthia[b]

[a]Department of Civil Engineering, King Mongkut Institute of Technology, North Bangkok, 1518 Pibulsongkram Road, Bangsue, Bangkok 10800, Thailand

[b]Department of Civil Engineering, University of British Columbia, 2324 Main Mall, Vancouver, BC, Canada V6T 1Z4

Received 1 February 2002; accepted 4 May 2004

Abstract

The effect of confinement on plain and fibre-reinforced concrete (FRC) prisms subjected to uniaxial compressive impact was studied. It was found that the response of the material changed with the degree of confinement. Confined concrete exhibited more ductile behaviour, with both strength (f_c') and ultimate strain (ε_{ult}) increasing with the degree of confinement. However, the elastic modulus (E) of the confined specimens was found to be about the same as or slightly lower than those of unconfined prisms. In addition, the relationship between stress and stress rate (n value) was also determined. It was found that, with confinement, the material became more rate sensitive.

Keywords: Compressive strength; Elastic modulus; Impact; Mechanical properties

1. Introduction

Concrete is known to be a strain-rate-sensitive material; its properties change with changes in the rate of loading. Many studies [1–3] have shown that the apparent strength and the corresponding strain increase with increasing rate of loading. In most research studies, concrete specimens were subjected to simple loading conditions, such as uniaxial tension or compression or three-point bending. However, in practice, concrete may be subjected to much more complicated multiaxial loading. Many research studies have been carried out on concrete subjected to multiaxial loading, but mostly under only static loading conditions [4–10]. Therefore, our knowledge of the impact behaviour of concrete under confining stress is still far from complete. In this study, the compressive impact behaviour of plain and fibre-reinforced concrete (FRC) under confinement was examined, with a focus on the response of the material and its resulting mechanical properties.

2. Experimental procedures

Concrete with mix proportions of 1.0:0.5:2.0:2.5 (cement:water:sand:coarse aggregate), providing an average compressive strength of 44.5 MPa for plain concrete and 45.1 MPa for FRC, was prepared in the form of rectangular prisms of dimensions 100 × 100 × 175 mm. The concrete was mixed using a pan-type mixer, placed in oiled PVC forms in a single layer, roughly compacted with a shovel, and finally vibrated on a vibrating table before being covered with polyethylene sheets. After 24 h, the specimens were demoulded and transferred to storage in a lime-saturated water tank for 30 days. Hooked end steel fibres were used (Table 1) at volume fractions of 0.5% and 1.0%.

An instrumented, drop-weight impact apparatus, designed and constructed in the Department of Civil Engineering, University of British Columbia, with the capacity of dropping a 578-kg hammer from heights of up to 2500 mm on the target specimen, was used to carry out the impact tests (see Ref. [11] for details of the impact machine). A load cell, 100 mm in diameter, with strain gauges mounted on it, was rigidly connected to the impact hammer.

An instrumented confinement apparatus was used to apply the lateral confinement stresses (Fig. 1). This appa-

* Corresponding author.

E-mail address: smindess@civil.ubc.ca (S. Mindess).

[1] This work was done while he was a PhD student at the University of British Columbia.

0008-8846/$ – see front matter © 2004 Elsevier Ltd. All rights reserved.
doi:10.1016/j.cemconres.2004.05.011

Table 1
Geometry of fibre

Type	Shape	Length (mm)	Cross section	Diameter (mm)
Hooked end		30	circular	d = 0.50

ratus consisted of two 50-ton hydraulic jacks and two load cells instrumented with four strain gauges each, oriented in the *x* and *y* axis directions. The load cells were placed opposite to the jacks on each axis. Four heavy steel blocks, rigidly connected to a base plate to prevent horizontal displacement, were used to hold both the jacks and the load cells.

Two series of impact tests were carried out: (1) without confinement and (2) with confinement by steel platens. For both tests, the specimen was placed vertically on a 100×100-mm rigid steel base located at the center of the impact machine. The hammer was dropped from 250- and 500-mm heights to provide striking velocities of 2.21 and 3.13 m/s, with corresponding impact energies of 1417 and 2835 J, respectively. An accelerometer placed on the top of the hammer was used to determine the specimen deformation. For the confined tests, the confining stresses were varied from 0 to 1.25 MPa. Full details of the testing program are given in Table 2.

3. Results and discussion

3.1. Stress–strain response

The confinement stresses used in this study were completely unconfined, 0 (passive confinement), 0.625, and 1.25 MPa. For the latter three cases, since the specimens would all tend to expand laterally under compressive loading, the lateral confinement stresses would have increased somewhat during the impact event. Unfortunately, with the present test arrangement, it was not possible to measure these increases. They would, in

Table 2
Testing program

Designation	Description	Vf (%)	Drop height (mm)	Confinement stresses (MPa)
Unconfined tests				
CPL250	Plain	–	250	
CPL500	Plain	–	500	
C05HE250	FRC	0.5	250	
C05HE500	FRC	0.5	500	
C1HE250	FRC	1.0	250	
C1HE500	FRC	1.0	500	
Confined tests with steel platens				
CPL25B21.25S	Plain		250	1.25
CPL25B0.625S	Plain		250	0.625
CPL25B0S	Plain		250	0
CPL50B0.625S	Plain		500	0.625
CPL50B0S	Plain		500	0
C05H25B1.25S	FRC	0.5	250	1.25
C05H25B0.625S	FRC	0.5	250	0.625
C05H25B0S	FRC	0.5	250	0
C05H50B0.625S	FRC	0.5	500	0.625
C05H50B0S	FRC	0.5	500	0
C1H25B0.625S	FRC	1	250	0.625
C05H25B0S	FRC	1	250	0
C1H50B0.625S	FRC	1	500	0.625
C05H50B0S	FRC	1	500	0

any case, have varied along the length of the specimen during an impact event due to the reflections of the stress waves from the confined boundaries of the specimen. The typical responses of plain and FRC prisms are given in Figs. 2–4. The response of the confined concrete was quite similar to that of unconfined concrete; the prepeak response consisted of both linear and nonlinear portions, followed by a postpeak response (the descending branch). However, the confined specimens behaved in a more "ductile" manner with increasing confinement, as indicated by the increasing strain at peak load and toughness; the ultimate strength also increased. There was no direct relationship between the confinement stress and the elastic modulus. The responses of both plain concrete and FRC were quite similar, except that the toughness of

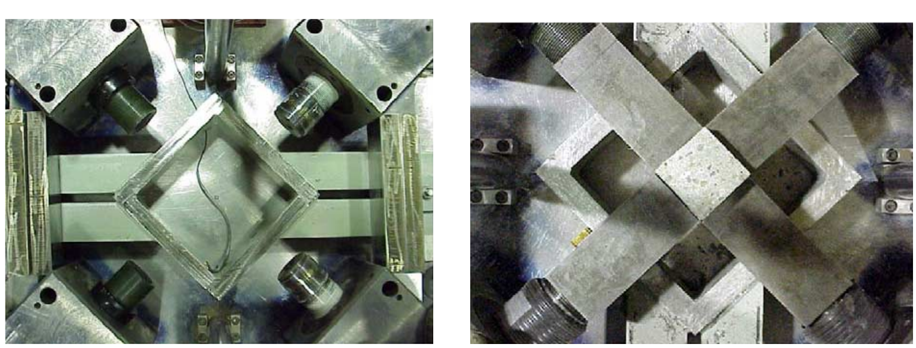

(a) Top view (b) Test setup

Fig. 1. Instrumented confinement apparatus.

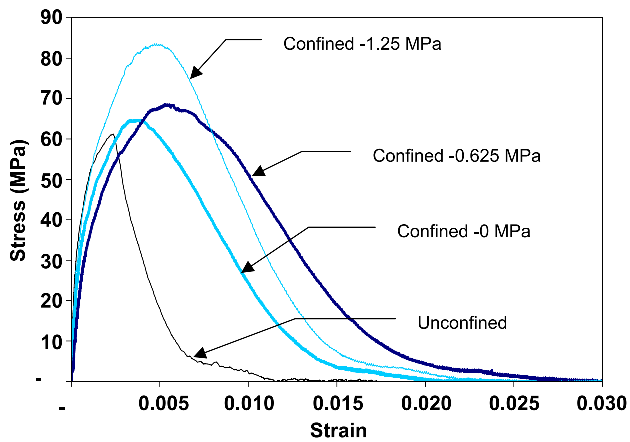

Fig. 2. Effect of confinement on compressive impact response of plain concrete prisms.

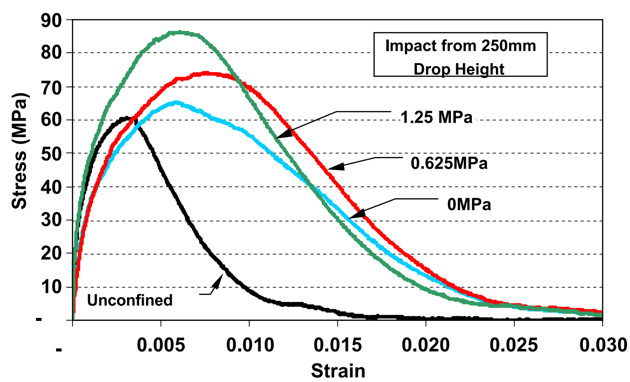

Fig. 3. Effect of confinement on compressive impact response of 0.5% HE FRC prisms.

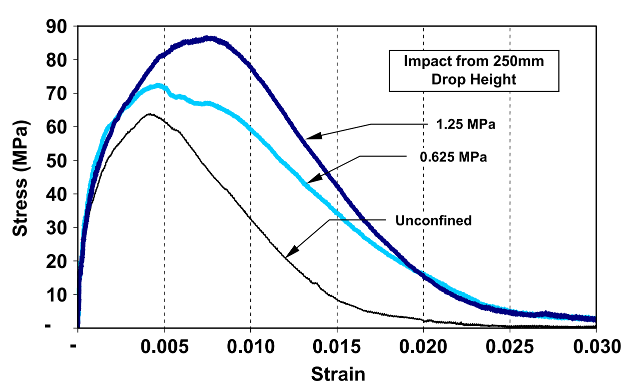

Fig. 4. Effect of confinement on compressive impact response of 1% HE FRC prisms.

Table 4
Confined/Unconfined strength ratios of plain and FRC prisms under impact

Concrete type	Drop height				
	250 mm			500 mm	
	0 C/U	0.625 C/U	1.25 C/U	0 C/U	0.625 C/U
Plain	0.95	1.01	1.23	1.09	1.15
0.5% HE	1.01	1.22	1.25	1.04	1.22
1.0% HE	1.03	1.24	–	1.03	1.22

0 C/U = ratio between 0 MPa confined and unconfined strength.
0.625 C/U = ratio between 0.625 MPa confined and unconfined strength.
1.25 C/U = ratio between 1.25 MPa confined and unconfined strength.

the plain concrete was, as expected, less than that of the FRC.

3.2. Compressive strength (f_c')

The apparent strength was found gradually to increase with the degree of confinement, as shown in Tables 3 and 4. Under "passive" confinement (0 MPa) and an impact energy of 1417 J, the increase in strength was quite small, about 0–5%. As the confinement increased to 0.625 and 1.25 MPa, the confined strength levels increased by 1–26% and 23–40%, respectively, compared with the unconfined strength. When the impact energy was doubled to 2835 J, the confined/unconfined (C/U) strength ratios did not change significantly.

The increase in strength of confined specimens is due, in part, to the friction between the fractured surfaces. Concrete always contains preexisting cracks and pores. Under stress, these "flaws" begin to propagate until one or several large cracks develop. At load levels above about 40% of the peak load, these cracks both grow in length and become wider, and the fracture surfaces begin to lose contact with each other. However, with the lateral confining pressure holding the fractured portions together, friction between the fracture surfaces may continue to support an axial load.

This behaviour may be explained by using the maximum normal strain theory of St. Venant [12]. As described above, the typical failure mode of the confined prisms was of a splitting or columnar type, with cracks running parallel to the direction of the applied impact load. This could imply that failure occurs when the lateral tensile strain (due to the Poisson effect) reached some critical

Table 3
Strength of confined plain and FRC prisms under impact loading

Concrete type	250-mm Drop height				500-mm drop height		
	Unconfined	Confinement stress (MPa)			Unconfined	Confinement stress (MPa)	
		0	0.625	1.25		0	0.625
Plain	65.80	62.67	66.52	80.92	81.02	85.97	90.81
0.5% HE	66.26	66.94	81.43	82.56	80.92	83.78	99.06
1.0% HE	70.51	72.40	86.50	–	85.76	88.01	105.02

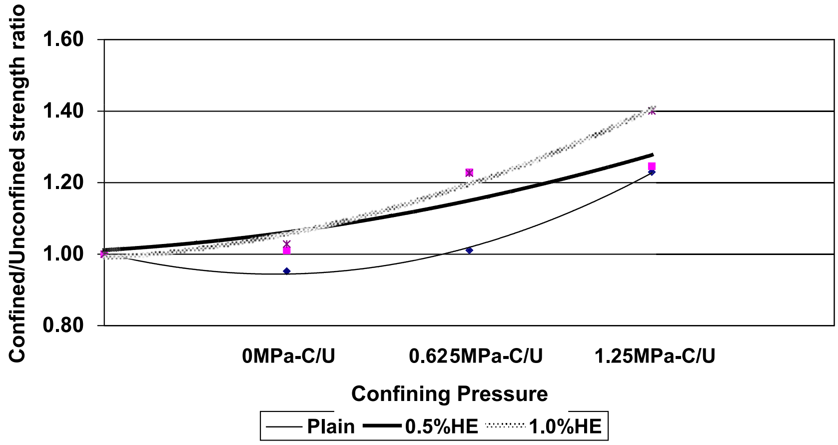

Fig. 5. Confined/Unconfined strength ratio of plain concrete and FRC.

value. That is, failure will occur in *unconfined* compressive impact when the lateral tensile strength σ_{tl} exceeds the tensile strength of concrete:

$$\sigma_{tl} \geq \sigma_t \quad (1)$$

However, using the St. Venant theory under *confined* compressive impact, it can be shown that failure will occur when:

$$\sigma_{tl} \geq \sigma_t - v(2\sigma_{con}) \quad (2)$$

where ν is the Poisson's ratio and σ_{con} is the lateral confining stress. Because this is compressive (i.e., negative using the normal sign convention), σ_{tl} under confinement must be greater than the lateral compressive stress in the unconfined state.

Different fibre contents provided different degrees of strength enhancement. The HE fibres at 1% by volume exhibited a higher C/U strength ratio (Fig. 5) than did either plain concrete or 0.5% HE at any confinement level. At 1.25-MPa confinement, the 1.0% HE FRC became so strong that failure did not occur.

3.3. Strain at ultimate stress (ε_{ult})

The strains at ultimate stress (ε_{ult}) of the confined prisms subjected to impact loading were found to increase with the degree of confinement by up to 87%, as shown in Table 5. However, the relationship between ε_{ult} and confinement was highly dependent on the fibre content and impact energy. Because the results show a high degree of scatter, there is no clear indication as to what fibre content would lead to a particular ε_{ult} at a given confinement and impact energy. In general, the effect of confinement on the ε_{ult} of plain concrete was larger than that of the FRC specimens. However, the absolute values of ε_{ult} were higher for the FRC specimens under similar conditions (Figs. 6 and 7). At the same degree of confinement, the ultimate strain increased with the rate of loading for both plain concrete and FRC.

3.4. Secant elastic modulus (E_s)

In this study, the secant modulus of elasticity was determined up to ultimate load (E_{sult}). For the confined prisms, E_{sult} appeared to decrease with increasing confinement by about 10% to 50%, depending upon the confinement, fibre content, and the impact energy. There was, however, a high degree of scatter in these data, particularly for low values of confining stress. At higher levels of confinement, both E_{sult} and degree of scatter decreased, as shown in Figs. 8 and 9. This effect is opposite to that found by Vile [6], who found that E_s increased with increasing confinement. The reasons for this difference are not clear. It may be related to the fact that Vile's work was carried out under static loading conditions, while in the present study, the results were obtained under impact. It may also be that in the present work, the displacements determined by mounting the accelerometer on the impact hammer rather than on the specimen itself led to unrealistically high apparent deformations and therefore lower modulus values. This aspect warrants further investigation.

Table 5
Ultimate strains of confined plain and FRC under impact loading

Concrete type	Hammer drop height (mm)	Unconfined ult. strain	Confined ult. strain		
			0 MPa	0.625 MPa	1.25 MPa
Plain	250	0.00212	0.00407	0.00519	0.00543
Plain	500	0.00239	0.00505	0.00601	–
0.5% HE	250	0.00375	0.00429	0.00593	0.00686
0.5% HE	500	0.00383	0.00549	0.00631	–
1% HE	250	0.00413	0.00535	0.00648	0.00702
1% HE	500	0.00398	0.00729	0.00703	–

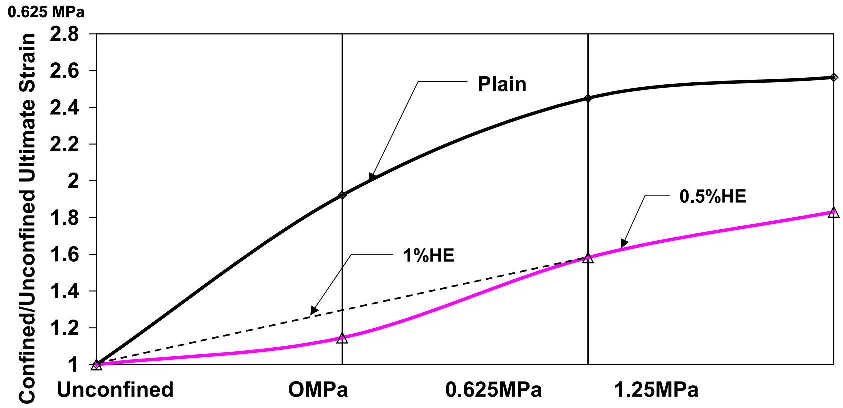

Fig. 6. Effect of confinement on relative ultimate strain at ultimate stress (impact from 250 mm).

3.5. Relationship between stress and stress rate

By assuming a linear relationship between stress or strain and the time to the peak load, the average stress or strain rates can be calculated as follows:

$$\text{Stress rate}(\dot{\sigma}) = \frac{\sigma_c'}{t_{ult}} \tag{3}$$

where σ_c' = ultimate stress (MPa) and t_{ult} = time to reach the ultimate stress (s).

It is well known (e.g., Ref. [3]) that strength may be related to stress rate by the following equation:

$$log\sigma_f = C + \frac{1}{n+1} log\dot{\sigma} \tag{4}$$

where σ_f = failure stress (MPa), $\dot{\sigma}$ = stress rate (MPa/s), C = empirical constant, and $1/n$ = slope of the curve of log strength versus log stress rate.

To determine n, the experimentally obtained relationships between $\log(\dot{\sigma}_f)$ and $\log(\dot{\sigma})$ were plotted (Fig. 10). Due to the lack of data in the intermediate range between static and impact loading, the plots were made using the impact data only. The best fit straight line for each data set was used to determine the slope and, hence, n. The n values found in this study ranged between 4.61 and 4.79 for the unconfined tests, with both plain concrete and FRC exhibiting essentially the same n values.

Theoretically, the n value should indicate the rate sensitivity ·of the material. As the slope of the $\ln\sigma_f$ versus $\ln\sigma$ plot increases, the n value decreases; the lower the n value, the higher the rate sensitivity. In the work of Banthia [3], n values as low as 1.25 were obtained. However, his work was carried out on beam specimens, and it is generally found that concrete in flexure is more rate sensitive than in compression. Thus, higher values of n were found in the present work for unconfined specimens.

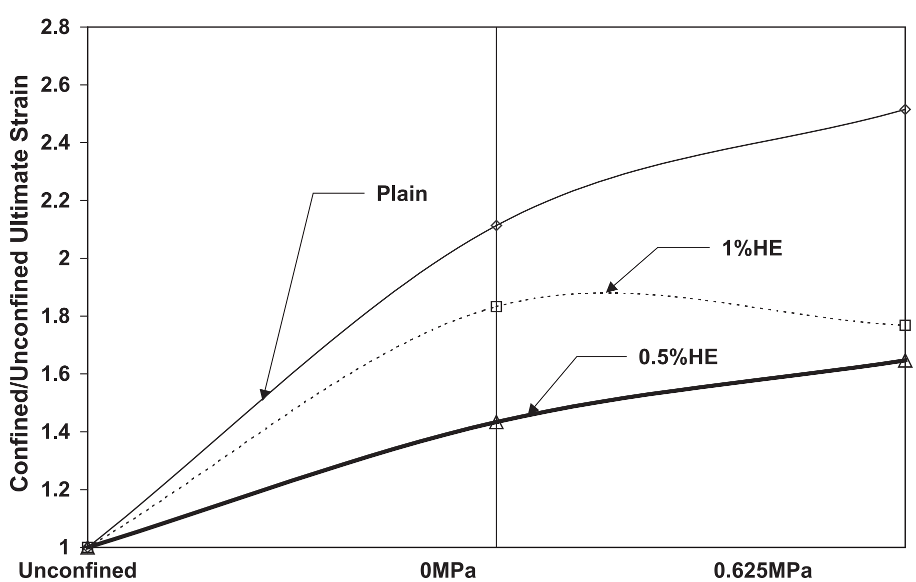

Fig. 7. Effect of confinement on relative strain at ultimate stress (impact from 50 mm).

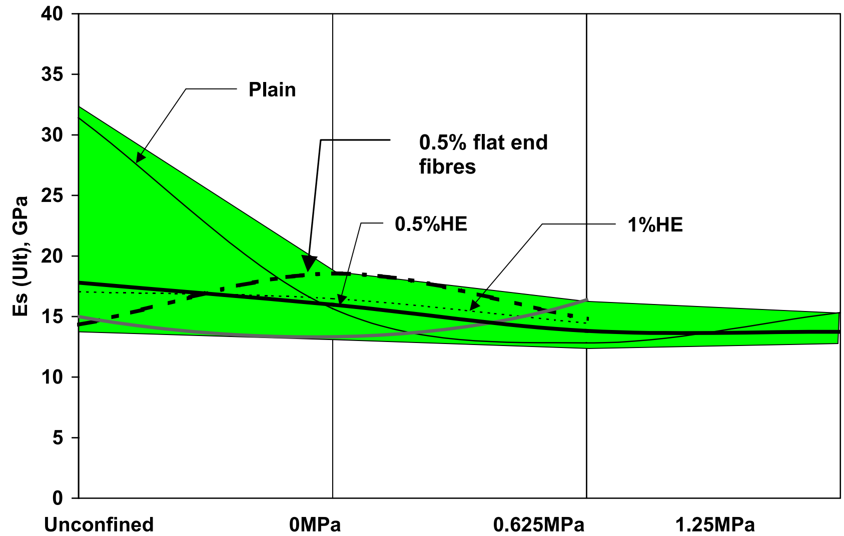

Fig. 8. Confined E_{sult} under impact loading (250-mm drop height).

The confined concrete, however, was more stress rate sensitive than the unconfined concrete, as may be seen by the steeper slopes and the lower n values of the curves (Table 6).

As previously stated, the smaller the value of n, the higher the rate sensitivity. It has been found here that the n value dropped significantly with increasing confinement stress, especially for plain concrete. This suggests that confined concrete is more rate sensitive than unconfined concrete is. Unlike the unconfined tests, fibres had a substantial effect on the n values in the confined tests. It was found that the rate of decrease in n values for FRC was lower than in plain concrete (Table 6). This indicates that confined FRC is less rate sensitive than confined plain concrete is. In addition, it was also observed that the n values of FRC at each confining stress were higher than those of plain concrete.

The apparently higher rate sensitivity of confined compared with unconfined concrete, as indicated by the much lower n values of the confined specimens, may be related to the differences in failure patterns. As shown in Fig. 11, the unconfined concrete failure pattern was characterized by diagonal “shear” cracks, while that of the confined concrete was characterized by vertical splitting tension cracks, parallel to the direction of loading. This suggests that the so-called unconfined specimens were probably confined by friction at the ends and were not under truly uniaxial compression. Because of aggregate interlock and the roughness of the fracture surfaces, it is likely that the inclined cracks in the unconfined case could not propagate as easily as in the vertical direction, leading to higher n values.

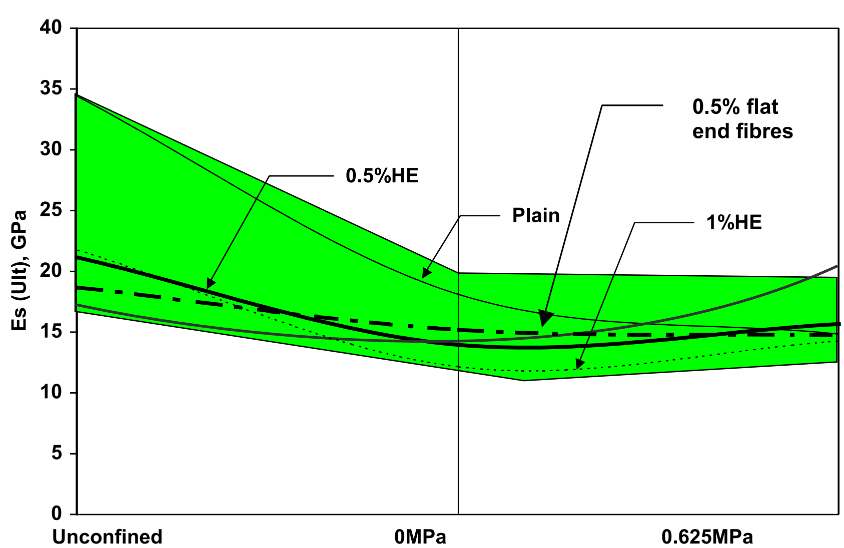

Fig. 9. Confined E_{sult} under impact loading (500-mm drop height).

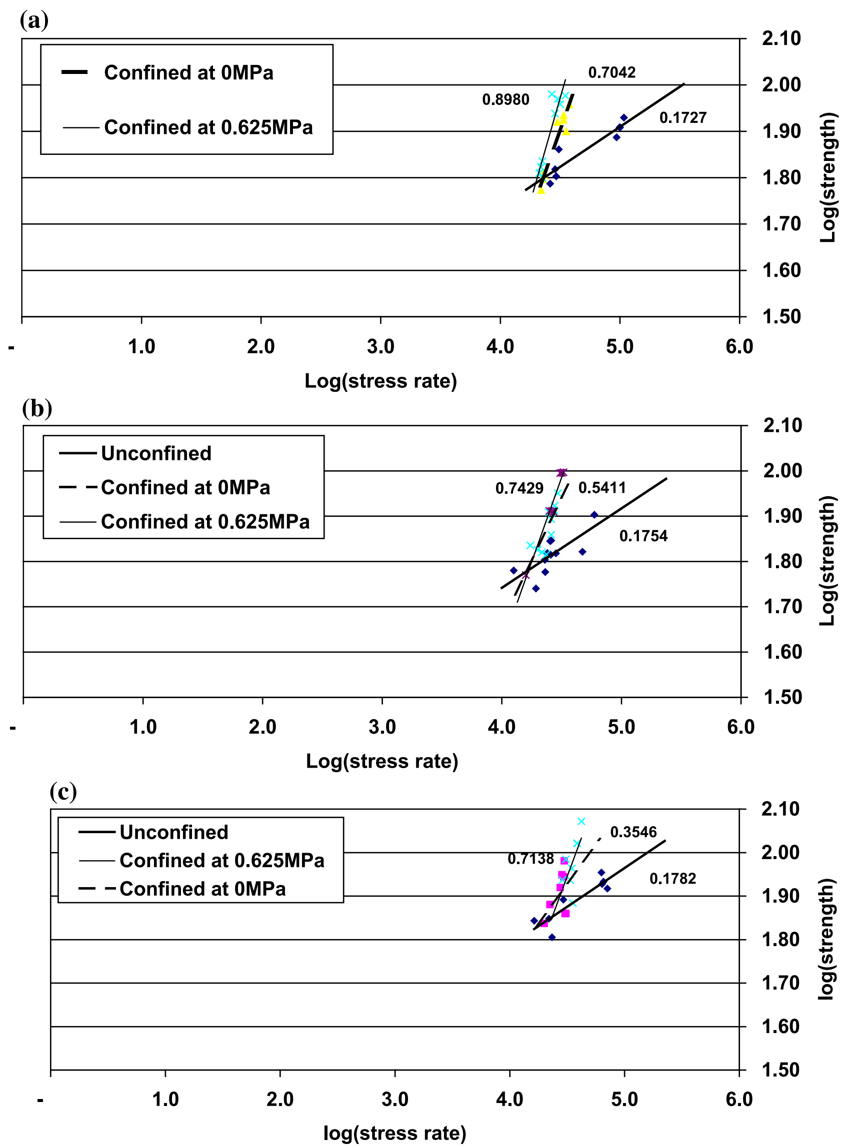

Fig. 10. Relationship between stress rate and strength of confined (a) plain concrete, (b) 0.5% HE FRC, and (c) 1.0% HE FRC.

The larger n values for the FRC compared with the plain concrete are easier to explain. They are due to the bridging effects of the fibres across the cracks, which tend to inhibit crack growth and lend to significantly lower crack velocities, as shown in Ref. [3].

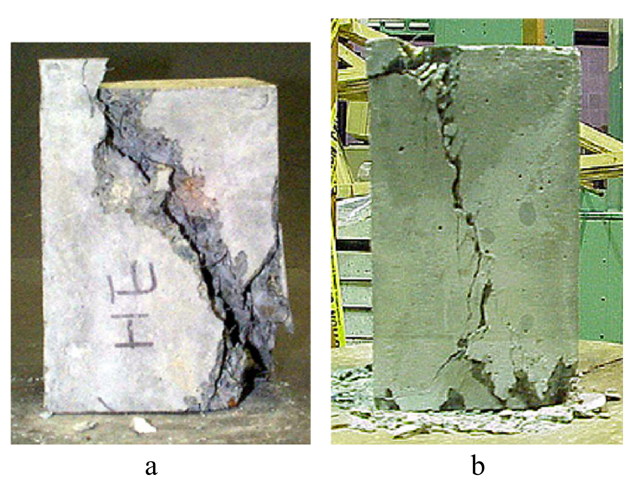

Fig. 11. Failure patterns of prisms subject to impact loading: (a) Diagonal shear failure (1% HE FRC-unconfined–500-mm drop height) and (b) splitting failure (0.5% HE FRC-confined—250-mm drop height).

Table 6
Slopes and n values of unconfined and confined concretes

Concrete type	Unconfined		Confined at 0 MPa		Confined at 0.625 MPa	
	Slope	n Value	Slope	n Value	Slope	n Value
Plain	0.173	4.79	0.704	0.42	0.898	0.11
0.5% HE FRC	0.175	4.70	0.541	0.85	0.743	0.35
1% HE FRC	0.178	4.61	0.355	1.82	0.714	0.40

4. Conclusions

1. Confinement affects the mechanical properties of concrete. In general, the ultimate strength and corresponding strain increased with increasing confinement.
2. The secant modulus of elasticity appeared to decrease somewhat under increasing confinement.
3. Confined concrete exhibited a higher rate sensitivity than unconfined concrete, as shown by the lower values of n.

Acknowledgements

The authors wish to thank Natural Science and Engineering Research Council of Canada (NSERC) for financially support this research and Mr. Max Nazar for designing and constructing the confinement apparatus.

References

[1] W. Suaris, S.P. Shah, Properties of concrete subjected to impact, J. Struct. Eng., Proc. ASCE 109 (ST7).

[2] D.L. Birkimer, R. Linderman, Dynamic tensile strength of concrete materials, ACI J. (1971) 47–49.

[3] N. Banthia, Impact Resistance of Concrete, PhD Thesis, University of British Columbia, Vancouver, Canada, 1987.

[4] K. Newman, Criteria for the behaviour of plain concrete under complex states of stress, The Structure of Concrete and Its Behaviour Under Load, Cement and Concrete Association, London, 1968, pp. 255–274.

[5] J.G.M. van Mier, Fracture Processes of Concrete, CRC Press, Boca Raton, FL, 1996.

[6] G. Vile, The strength of concrete under short-term static biaxial stress, The Structure of Concrete and its Behaviour Under Load, Cement and Concrete Association, London, 1968, pp. 275–288.

[7] H. Rusch, Physical problems in the testing of concrete, Zem.-Kalk-Gips 12 (1) (1959) 1–9.

[8] L.M. Laddie, R. Zimmerman, Compressive strength of plain concrete under multiaxial loading conditions, ACI J. 67 (10) (1970) 802–807.

[9] H. Kupfer, H. Kilsdorp, H. Rusch, Behavior of concrete under biaxial stresses, ACI J. 66 (8) (1969) 656–666.

[10] J.B. Newman, Concrete under complex stress, in: F.D. Lydon (Ed.), Developments in Concrete Technology—1, Applied Science Pub, London, 1979, pp. 151–219.

[11] N. Banthia, S. Mindess, A. Bentur, M. Pigeon, Impact testing of concrete using a drop-weight impact machine, Exp. Mech. 29 (2) (1984) 63–69.

[12] J.A. Collins, Failure of Materials in Mechanical Design, John Wiley and Sons, New York, 1981.